Electron Microscopy of Cytochrome *c* Oxidase Crystals: Labeling of Subunit III with a Monomaleimide Undecagold Cluster Compound†

J. Crum,‡ K. J. Gruys,§,|| and T. G. Frey*,‡

Department of Biology and Molecular Biology Institute, San Diego State University, San Diego, California 92182-4614, and Institute for Enzyme Research, University of Wisconsin—Madison, Madison, Wisconsin 53706

Received July 7, 1994; Revised Manuscript Received September 12, 1994®

ABSTRACT: Two-dimensional crystals of beef heart mitochondrial cytochrome *c* oxidase dimers were labeled at Cys-115 of subunit III with a monomaleimide derivative of an undecagold cluster compound. The binding site of the gold cluster compound and hence the site of subunit III were identified by image processing of cryoelectron micrographs of the crystals preserved in a mixture of glucose and uranyl acetate. The shape of the cytochrome oxidase dimer can be approximated as a parallelogram which is 44 by 82 Å with an included angle of 80° oriented with its long dimension along the *a* axis of the crystal. Labeling of subunit III was confirmed by a shift in the mobility of approximately 50% of subunit III molecules upon electrophoresis in polyacrylamide gels in the presence of sodium dodecyl sulfate. Averaged images of undecagold cluster labeled crystals and of unlabeled crystals were calculated; each image represents an average of approximately 17 000 molecules of either labeled or unlabeled cytochrome oxidase. On the basis of a statistical analysis of the differences between the two images, the gold cluster binds along a line 30° from the *a* axis and 29 Å from the center of the dimer. This result is interpreted in the context of other structural studies including the site of cytochrome *c* binding which Frey and Murray found to be near the *a* axis and 18 Å from the center of the dimer [Frey, T. G., & Murray, J. M. (1994) *J. Mol. Biol. 237,* 275−297]. A structural model is proposed with subunit III polypeptides near the *a* crystal axis approximately 30 Å from the center of the dimer and the subunit I and II polypeptides (which bind both hemes, *a* and a_3, and copper centers, Cu_A and Cu_B) near the center of the dimer.

Cytochrome *c* oxidase is the terminal electron transport complex (complex IV) of mitochondrial electron transport catalyzing the reduction of O_2 using electrons derived from the electron transport chain and delivered by ferrocytochrome *c* as shown by eq 1:

$$4 \text{ ferrocytochrome } c + 4H^+ + O_2 \rightarrow 4 \text{ ferricytochrome } c + 2H_2O \quad (1)$$

The four protons are consumed from the matrix space and an additional four protons are transported from the matrix to the intermembrane space (Wikstrom, 1977; Wikstrom et al., 1981). The scalar consumption and the vectorial pumping of protons by cytochrome *c* oxidase contributes to the creation of an electrochemical proton gradient across the membrane, which provides energy for synthesis of ATP by the mitochondrial ATP synthetase [for reviews see Capaldi (1990a,b), Haltia and Wikstrom (1992), and Saraste et al. (1991)].

As isolated from vertebrate mitochondria, cytochrome *c* oxidase consists of 13 distinct polypeptide subunits at unit stoichiometry, two heme *a* moieties (heme *a* and a_3), and two copper ions (Cu_A and Cu_B) with a molecular weight of 202 000 calculated from the polypeptide sequences (Buse et al., 1985; Kadenbach et al., 1983). When purified in detergent-solubilized form from beef heart mitochondria, cytochrome *c* oxidase may exist as either a monomer (13 polypeptides, 4 metal centers, and a molecular weight of 202 000) or as a dimer (molecular weight of 404 000), and both forms are active in catalyzing the reaction shown in eq 1 (Georgevich et al., 1983; Nalecz et al., 1983; Robinson & Talbert, 1986; Suarez et al., 1984). It is not known whether the active form of cytochrome *c* oxidase *in vivo* is a monomer, a dimer, or whether both forms are present.

Knowledge of the three-dimensional structure of cytochrome oxidase comes primarily from electron microscopy of two-dimensional crystals which are only one unit cell thick [for a review, see Frey (1994)]. Two such crystal forms have been reported, one consisting of dimers embedded in the phospholipid bilayers of large collapsed vesicles (Henderson et al., 1977) and a second consisting of sheets of cytochrome oxidase monomers without a continuous lipid bilayer (Fuller et al., 1979). The dimer crystal form has been the most extensively studied. Three-dimensional reconstructions calculated from electron micrographs of tilted crystals reveal a very asymmetric distribution of protein mass across the membrane, 50−60 Å on the inside of the collapsed vesicles and only 20 Å on the outside (Deatherage et al., 1982b; Valpuesta et al., 1990). Subunit specific antibodies identified the exterior surface as corresponding to the matrix or M-side of the inner mitochondrial membrane; thus, the inside surface of the vesicles, where cytochrome oxidase

† This work was supported by grant DMB-9019785 from the National Science Foundation to TGF and DK 28706 from the National Institutes of Health to Perry A. Frey. K.J.G. was supported by a postdoctoral research service award from the National Institute of General Medical Sciences, Grant GM10816.

‡ San Diego State University.

§ University of Wisconsin—Madison.

|| Present address: Monsanto Agricultural Company, 700 Chesterfield Parkway North, St. Louis, Missouri 63198.

® Abstract published in *Advance ACS Abstracts,* October 15, 1994.

0006-2960/94/0433-13719$04.50/0

protrudes the most, must correspond to the side facing the intermembrane space also called the C-side (Frey et al., 1978). The three-dimensional models and freeze fracture replicas show that the two monomer halves of a dimer split apart on the C-side of the membrane forming a cleft (Costello & Frey, 1982; Deatherage et al., 1982a; Deatherage et al., 1982b; Frey et al., 1982; Valpuesta et al., 1990).

The three largest cytochrome oxidase subunits (I, II, and III) are mitochondrial in origin while all of the smaller subunits are synthesized cytoplasmically as precursors and imported into mitochondria. Only subunits I and II have defined functions; subunit I binds both hemes and Cu_B while subunit II binds Cu_A. The smaller cytoplasmically synthesized subunits are missing in homologous bacterial cytochrome *c* oxidases, but within vertebrate mitochondria some of these subunits seem to be somewhat tissue specific (Anthony et al., 1990). Subunit III, the third mitochondrially synthesized subunit, was first thought to constitute at least part of the proton pump; this proposal was later amended giving III a role in regulating proton pumping (Prochaska & Fink, 1987). A subsequent study indicates that subunit III plays a role in assembly of an intact complex (Haltia et al., 1989). Subunit III is one of relatively few cytochrome oxidase subunits which can be removed without markedly affecting enzyme activity (Nalecz et al., 1985; Robinson & Talbert, 1986; Thompson & Ferguson-Miller, 1983). Several studies, however, have suggested that subunit III may play a role in formation and/or stabilization of dimeric cytochrome oxidase, and there is some evidence to suggest that while cytochrome oxidase monomers are fully active in electron transport only dimers are capable of pumping protons (Finel & Wikstrom, 1986; Sone & Kosako, 1986).

Cys-115 of subunit III is the sulfhydryl in cytochrome oxidase most reactive to hydrophilic sulfhydryl reagents, and Cys-115 can be labeled selectively under appropriate conditions (McGeer et al., 1977; Hall et al., 1988; Malatesta & Capaldi, 1982; Muller & Azzi, 1985). Yang et al. (1984) have described the synthesis of an undecagold cluster compound containing a single maleimide group which can be used to label selectively cysteine sulfhydryl groups. Similar compounds have been prepared by other groups and have proven very useful in labeling sites on macromolecular assemblies for identification by electron microscopy (Hainfeld, 1988; Milligan et al., 1990; Safer et al., 1986; Yang et al., 1994). We report here the use of this compound to label Cys-115 of subunit III in two-dimensional crystals of cytochrome *c* oxidase dimers and the identification of the labeling site in two-dimensional projection by low dose electron microscopy. This result is interpreted in the context of previous studies of cytochrome oxidase structure including the proposed site of cytochrome *c* binding reported by Frey and Murray (1994). A preliminary report of this work has been presented at the Biophysical Society meeting in 1994 (Crum et al., 1994).

MATERIALS AND METHODS

Preparations. Cytochrome *c* oxidase crystals (dimer form) were prepared as described by Frey et al. (1978) except that peroxide-free Triton detergents were used; these were either prepared as described by Lever (1977) or purchased from Pierce Chemical Co. as 10% solutions sealed under nitrogen gas in glass ampules. Monomaleimide undecagold cluster was prepared as described by Yang et al. (1984).

Labeling: Cytochrome oxidase crystals were incubated at a concentration of 10 μM heme aa_3 with a 10-fold molar excess of monomaleimide undecagold cluster in 25 mM PIPES [piperazine-*N*,*N*'-bis(2-ethanesulfonic acid)] pH 7.0 for 1 h at room temperature and overnight in the refrigerator. A control sample was treated identically except that no gold cluster reagent was included in the incubation mixture. Crystals were separated by centrifugation in a microfuge and washed twice with twice the original volume of 25 mM sodium citrate (pH 6.8). The washed pellets were suspended in three times the original volume of sodium citrate buffer and homogenized with a small glass Teflon homogenizer. A portion of this sample was taken for analysis by SDS–PAGE[1] and the remainder frozen in liquid nitrogen and kept at −70 °C until used.

SDS–Polyacrylamide Gel Electrophoresis. SDS–PAGE was performed in 12.5% gels using the buffer system described by Kadenbach et al. (1983). This system provides the maximal separation of subunits II and III. The samples in citrate buffer were first pelleted in a microfuge, dissolved in sample buffer (without reducing agent), and heated in boiling water for 15 s before loading onto 1.5 mm thick slab gels. Gels were allowed to run until the bromphenol blue dye front reached the bottom of the gel. The gels were then fixed for 1 h in 10% trichloroacetic acid/50% methanol, stained for 1 h in 0.25% Coomassie Blue R250/50% methanol/7.5% acetic acid, and destained in several changes of 10% acetic acid/25% methanol (all at 35 °C with agitation). Gels were photographed by transillumination using a yellow filter to enhance contrast of the blue stained protein bands. Negatives were scanned with an Eikonix digitizing camera (see below) and images transferred to a Macintosh computer for analysis using the public domain program NIH Image 1.54 (Division of Computer Research and Technology, National Institutes of Health, Bethesda, MD 20892). Two methods were used for quantitation of gels. In the first method gel bands were isolated with a rectangular selection tool, and the average background intensity of a neighboring area was subtracted from each pixel within the selection area. The intensity of the band could then be estimated by summing the pixel values within the selection area. The second method is based on the method described in the documentation accompanying NIH Image 1.54 and the gel plotting macros. Briefly, a downward sloping baseline was drawn from the minimum to the left of peak I to the minimum between peaks VII and VIII. The peaks were then enclosed on both sides by vertical lines from the plot to the baseline and the enclosed area of each measured. For comparison of different lanes, the data were normalized so that the sum of the areas of all peaks was 100. When corresponding peaks in different lanes from the same gel were compared, each method produced results consistent all cases to within 15% with an average variation of 8%. Average integrated intensities for peaks quantitated by the first method agreed with the second method to better than 20% in all cases with an average variation between the two methods of 13%.

Electron Microscopy. Specimens were prepared by adsorption to glow discharged carbon films on 400 mesh copper

[1] Abbreviations: Au_{11}, undecagold cluster compound; NEM, *N*-ethyl maleimide; SDS–PAGE, sodium dodecyl sulfate–polyacrylamide gel electrophoresis.

grids and drying in a solution of 0.5% glucose/0.5% uranyl acetate as described by Valpuesta et al. (1990) Electron micrographs were recorded at 40 000× magnification in a Philips EM 410 electron microscope equipped with a Philips low dose exposure unit, a Gatan 626 cryospecimen holder, and a Gatan anticontamination device. Specimens were cooled to −170 °C after transfer to the microscope, and low dose electron micrographs were recorded on Kodak SO-163 film at 100 kV. Using the low dose exposure unit, focusing and astigmatism correction were adjusted on an area adjacent to crystals located by scanning at low magnification with negligible electron exposure. Thus, crystals were not exposed to appreciable electron radiation prior to recording the micrograph. Exposure was adjusted so that when the film was developed according to the manufacturer's instruction for maximal sensitivity (12 min in full strength D19 at 20 °C) a negative of acceptable density resulted. We estimate that this corresponds to an electron exposure of 10−15 electrons/Å^2. This procedure of specimen preparation was chosen as it had been found previously to produce the highest resolution electron micrographs of the dimer crystal form (Valpuesta et al., 1990).

Image Processing. Micrographs were selected for processing based upon optical diffraction patterns showing reflections to relatively high spatial frequency and proper focus and correction of astigmatism. Five micrographs of undecagold labeled crystals and five micrographs of control (unlabeled) specimens were selected for computer processing. Electron micrographs were scanned using an Eikonix Model EC 78/99 digitizing camera interfaced to an AT&T 80386 computer. Areas 1024 × 1024 pixels in size (12.5 μm pixels) were saved and transferred to either a VAXStation 3100 or Silicon Graphics Indigo computer workstation for further processing. Images were processed as described by Henderson et al. to correct for lattice distortions using software kindly provided by Dr. R. Henderson at the MRC Laboratory of Molecular Biology, Cambridge, England (Henderson et al., 1986). For each image, the symmetry of the two-dimensional space group, *pgg*, was imposed after translating the origin to the nearest 2-fold axis (Hahn, 1983). Phase origins of all images were adjusted to a common point by inspection of the images. Structure factor lists were scaled so that the sum of structure factor intensities was constant for all images before calculating average images within each group. Average images and difference images were calculated in Fourier space by adding or subtracting structure factors or in real space by using the SPIDER image processing system (Frank et al., 1981). The statistical significance of peaks observed in the difference image was determined by calculating a corresponding array of Student's *t*-values calculated for small samples as described by Milligan and Flicker using programs kindly supplied by Dr. R. Milligan (Milligan & Flicker, 1987). Images are displayed in grayscale with contrasting contour lines except for Figure 6.

RESULTS

After the first centrifugation, the samples incubated with monomaleimide undecagold cluster were orange; subsequent washing reduced the orange tint, but the pellet after the second wash was noticeably more orange than the control which retained a gray-green color. We were unable to quantitate the amount of gold cluster bound to the crystals by UV/vis spectrophotometry because of the low concentration, the turbidity of the samples, and the fact that the absorption bands of the undecagold cluster compound overlap the protein and heme Soret bands of cytochrome oxidase at 280 and 420 nm, respectively.

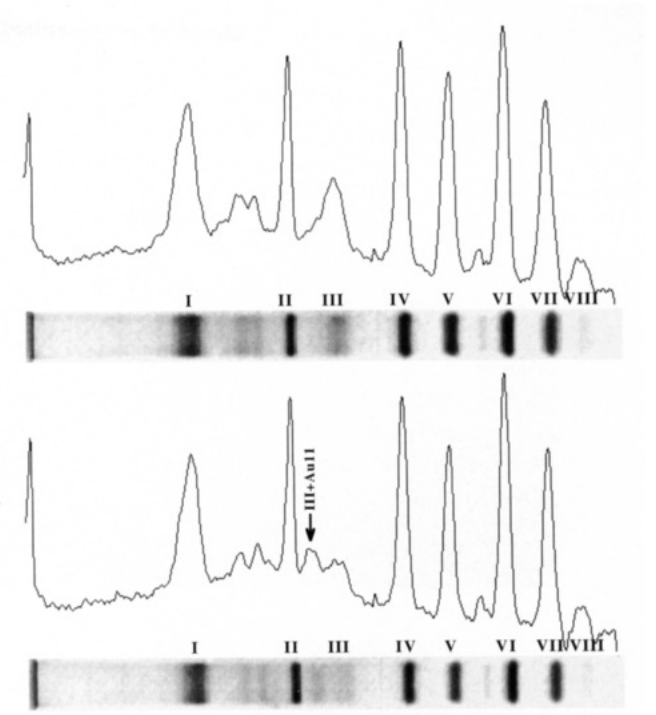

FIGURE 1: SDS−PAGE analysis of crystalline membranous cytochrome *c* oxidase samples. One gel lane is displayed horizontally with the top of the gel to the left; above each gel lane is a plot of staining intensities integrated perpendicular to the direction of migration. Bands corresponding to subunits I, II, III, IV, V, VI, VII, and VIII are indicated. Bands V, VI, and VII each contain multiple polypeptide species with similar molecular weights which are not resolved by this gel system. (a) Control sample. (b) Sample labeled with monomaleimide Au_{11}. The band corresponding to subunit III is diminished in intensity and a new band, subunit III with the Au_{11} bound to Cys-115 (III-Au_{11}), appears between subunits II and III.

SDS−PAGE. Figure 1 shows SDS polyacrylamide gels of both control and Au_{11}-labeled samples of cytochrome oxidase vesicle crystals used for structural analysis by low dose electron microscopy. The control sample displays bands typical of beef heart cytochrome oxidase samples although a number of the smaller subunits are not resolved on this gel. The bands corresponding to the three large mitochondrially synthesized subunits are labeled (I−III) and the cytoplasmically synthesized subunits are labeled IV−VIII. Bands V, VI, and VII each consist of multiple subunits which are not resolved in our gel system: band V contains subunits Va and Vb; VI contains VIa, VIb, Vc; VII contains VIIa, VIIb, and VIIc. The two weak bands between subunit I and II are contaminants commonly found in cytochrome *c* oxidase prepared from beef heart mitochondria, particularly in preparations of two-dimensional crystals.

Subunit III appears as a diffuse staining band which does not show up well in photographs of gels; this is typical of all preparations of cytochrome *c* oxidase. The integrated intensity of the subunit III band, however, is comparable to that of the subunit II band. The gel of the Au_{11}-labeled sample (Figure 1b) appears to be identical to the control sample except for the appearance of the subunit III band. In the Au_{11}-labeled sample the band corresponding to subunit

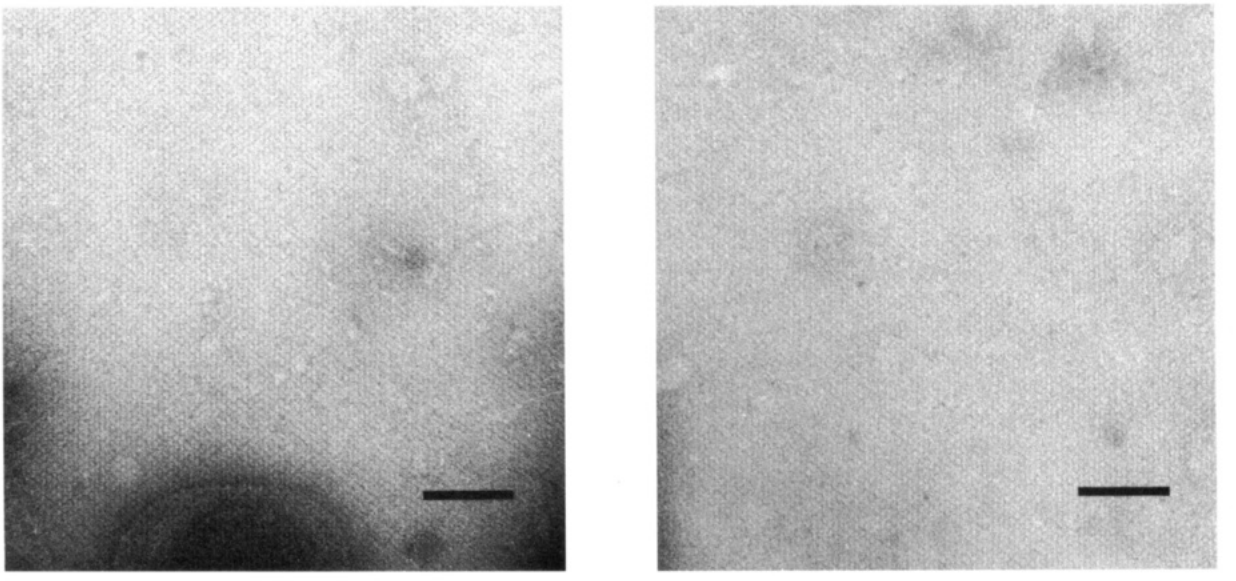

FIGURE 2: Electron micrographs of two-dimensional crystals of cytochrome oxidase dimers. The vesicular crystals are embedded in a mixture of glucose and uranyl acetate and low dose micrographs were recorded at −170 °C. (a) Control sample. (b) Sample labeled with monomaleimide Au_{11}. Scale bar indicates 100 nm.

III is diminished in intensity and a new diffuse band appears between the positions of subunit II and subunit III. Other studies using undecagold cluster compounds to label proteins also found that the gold cluster decreases the mobility of the protein to which it is bound by an amount corresponding to an increase in molecular weight of roughly 5000 daltons, the molecular weight of the gold cluster compound (Safer et al., 1986; Yang et al., 1994). Thus, we identify this band as subunit III with covalently bound Au_{11} based upon its higher apparent molecular weight.

McGeer et al. (1977) found that at pH 7.0, NEM labels only subunit III of detergent solubilized cytochrome oxidase when incubated at equal molar concentrations but will also label subunit VIa when NEM is present at 10-fold molar excess. However, they found that when membrane bound cytochrome oxidase (mitochondria or electron transport particles) was incubated with an excess of NEM, subunit III was labeled more strongly than in the case of solubilized enzyme, subunit VIa was not labeled at all, and subunit I was partially labeled but much less than III. Although our cytochrome oxidase molecules are membrane bound, we considered the possibility that subunit VIa is also labeled by Au_{11}. If VIa reacted with Au_{11}, it would be expected to migrate at a higher apparent molecular weight, approximately the molecular weight of subunit V. This would result in a decrease in the intensity of the band for subunits VIa,b,c and either the appearance of a new band with a lower mobility or an increase in the intensity of the subunits Va,b band. While we found a small decrease in the area of the peak for VIa,b,c from 17.4% of the total peak area to 16.9%, the area of the peak for Va,b also decreased from 13.9% to 11.3%. Both changes are within the experimental error of our methods. Since we also did not see a new peak appearing which might correspond to a VIa-Au_{11} species, we conclude that subunit VIa does not react with the monomaleimide undecagold cluster reagent.

The integrated intensities of the two subunit III bands in the Au_{11}-labeled sample (III and III-Au_{11}) indicate that approximately 50% of subunit III has reacted with monomaleimide undecagold cluster. The area under the subunit III peak in the control sample was 8.1% of the area under all peaks while in the Au_{11}-labeled sample the subunit III peak was 3.7% and the III-Au_{11} peak was 4.1% of the total. For comparison, the subunit II peak is about 11% of the total and the average standard deviation of peak intensities for all bands in four different gel lanes was ±1% of the total area. Thus, within experimental variation all of the intensity of the subunit III band in the control sample is accounted for by the two subunit III bands in the Au_{11}-labeled sample. The splitting of the subunit III band into two with the new band at higher apparent molecular weight is reproducible, and in other Au_{11}-labeled specimens we have confirmed the presence of gold atoms in individual crystals of cytochrome oxidase by energy dispersive X-ray analysis (data not shown).

Electron Microscopy. Figure 2 shows typical electron micrographs of control and of Au_{11}-labeled crystals. The crystals were prepared by embedding in 0.5% glucose/0.5% uranyl acetate, and are therefore negatively stained. The resolution of the micrographs, based upon Fourier transforms of images which had been corrected for lattice distortions, was approximately 15 Å. This is not as good as previously obtained but proved to be adequate to identify the site of Au_{11} binding to subunit III. Figure 3 compares the averages of the five best electron micrographs of both control (Figure 3a) and Au_{11}-labeled (Figure 3b) cytochrome oxidase crystals. Each of these images represents the average of over 4000 unit cells (approximately 17 000 molecules) in five electron micrographs of each sample. There are only subtle differences in these images, but in hindsight the effects of Au_{11} binding can be discerned. Since the samples are negatively stained, adding a heavy atom cluster should darken the image, and, indeed, the Au_{11}-labeled image is somewhat denser at the ends of the dimers along the *a* axis. This is most evident when the second black contour lines are compared.

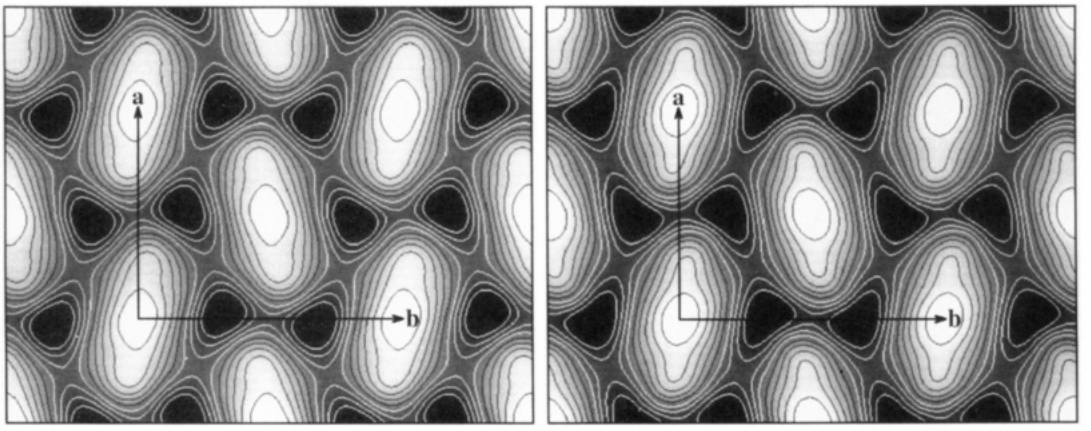

FIGURE 3: Average projection images from cryoelectron micrographs (a) of the control sample and (b) of the crystals labeled at Cys-115 of subunit III with monomaleimide Au_{11} compound. Each image represents the average of over 4000 unit cells (17 000 molecules) in the five best images of each sample. The *a* (97 Å) and *b* (125 Å) crystal axes are indicated.

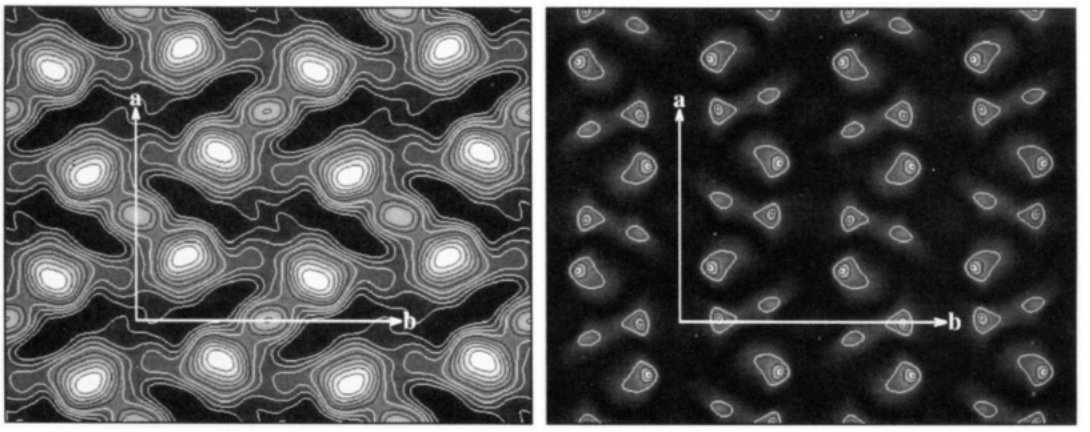

FIGURE 4: (a) Difference image calculated by subtracting Figure 3b (Au_{11}-labeled sample) from Figure 3a (control sample); thus, the lighter areas correspond to extra electron density from the Au_{11} compound. One significant difference peak is found per monomer (two per dimer) at five contour levels above the baseline; these correspond to Au_{11} compound bound to subunit III via Cys-115. (b) Map of Student's *t* values or "*t*-map" in which each pixel contains a *t* value calculated from the 10 images used in this study (five images of the control sample images and five images of the Au_{11} labeled sample). The contour lines begin at a $t = 2$ indicating significance at the 5% confidence level for eight degrees of freedom with the highest contour level at $t = 5$ corresponding to significance at the 0.1% confidence level (i.e. the probability of this difference arising by chance is 0.1%). Crystal axes *a* and *b* are indicated.

Difference Image. The presence of the Au_{11} label is seen clearly in the difference image in Figure 4a. The difference image was calculated by subtracting the image of the Au_{11}-labeled sample from the image of the control sample so that the position of the undecagold cluster would appear as lighter areas which we will define as positive difference peaks. The difference image indeed contains one prominent and well-defined positive difference peak per asymmetric unit (i.e., one peak per cytochrome oxidase monomer or two per dimer). This peak is five contour levels above background compared to one diffuse and ill-defined negative difference peak at four contour levels below background. There are only two other positive peaks, and they are much weaker at only three and two contour levels above background.

We analyzed the statistical significance of the difference image by calculating a corresponding image of Student's *t* values. Given the number of degrees of freedom as 8 (the total number of images, 10, minus the number of groups, 2), a *t* value of 2.3 indicates that the difference between samples is significant at the 5% confidence level. The pixels in the "*t*-map" shown in Figure 4b correspond point for point with the pixels of the control sample image (Figure 3a), the Au_{11}-labeled sample image (Figure 3b), and the difference image (Figure 4a). The contour lines start at a *t* value of 2, and the highest contour level outlines an area of the map where the *t* value is greater than 5 which for 8 degrees of freedom indicates a difference significant at the 0.1% confidence level (i.e., the probability that the difference observed in this region of the map is due to chance alone is less than 0.1%). The region with the highest *t* value (greater than 5) occurs within the highest positive difference peak indicating that it is highly significant. The only other areas of the "*t*-map" with a magnitude of 2 or higher are in negative areas of the difference map and could not, therefore, correspond to the position of Au_{11} binding. Figure 5 is the average image of unlabeled crystals with the difference peak and the highest peak in the "*t*-map" overlaid. The peak in the "*t*-map" lies on the cytochrome oxidase dimer 29 Å from the center of the molecule along a line 30° from the *a* axis, and this is likely the location of the gold cluster.

DISCUSSION

The function of cytochrome oxidase subunit III has been debated for a number of years. It was initially thought to

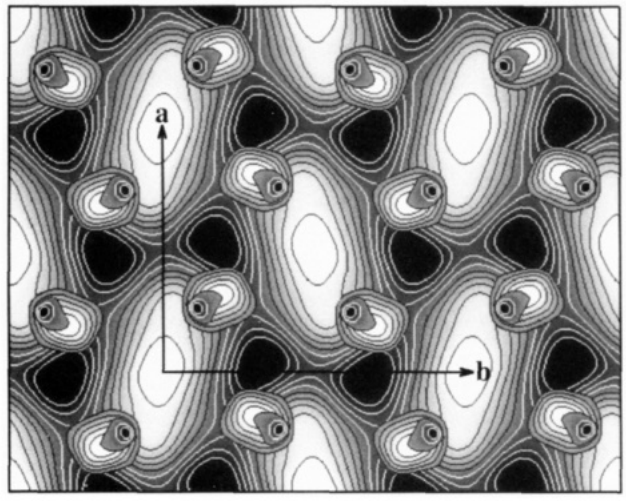

FIGURE 5: Image of the control sample with the positive difference peak and the peak in the *t*-map overlaid. The *t*-map peak is not centered in the difference peak but lies to one side where the difference peak overlaps the protein stain-excluding domain 29 Å from the center of the cytochrome oxidase dimer. Crystal axes *a* and *b* are indicated.

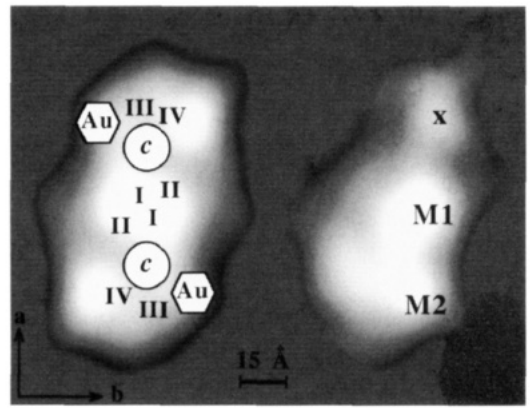

(a) (b)

FIGURE 6: (a) Image of a single cytochrome oxidase dimer calculated from electron micrographs of frozen hydrated crystals. The site of Au_{11} binding is indicated based upon the positions of *t*-map peaks in Figure 5 along with the site of cytochrome *c* binding published by Frey and Murray (1994). The *approximate* locations of subunits I, II, III, and IV are shown as discussed in the text. (b) Image of a single cytochrome oxidase monomer calculated from electron micrograpahs of frozen hydrated crystals (Frey & Murray, 1994). The image has been rotated to the orientation it would have in the dimer shown in Figure 6a so that the correspondence between monomer domains M1, M2, and X and the domains of the dimer can be inferred (Fuller et al., 1979).

comprise the proton pump, but later work revised this role to regulation of proton pumping activity (Prochaska & Fink, 1987). More recently Haltia et al. (1989, 1991) have suggested that subunit III facilitates assembly of the other subunits. Finel has suggested that subunit III also stabilizes the dimeric form of the enzyme (Finel, 1989; Finel & Wikstrom, 1988). We have identified the site of a maleimide undecagold cluster derivative linked covalently to subunit III, presumably to Cys-115. Based upon the most significant difference in the labeled vs control images, the gold cluster lies on a line 30° from the *a* crystal axis 29 Å from the center of the dimer. Cys-115 of subunit III could be as much as 15 Å (the 10 Å radius of the undecagold cluster compound plus an estimate of the length of the arm containing the reactive maleimide) from the gold cluster locus, but the 15 Å separation would occur in these projection images only if the arm connecting the maleimide moiety to the gold cluster core were fully extended parallel to the plane of the bilayer in which the crystals form. In higher resolution images two-dimensional projections of cytochrome oxidase dimers display three major peaks of density, a central domain around the 2-fold axis and two equivalent peripheral domains lying along the *a* crystal axis approximately 30 Å from the center of the dimer (Frey & Murray, 1994; Valpuesta et al., 1990). As shown in Figure 6a, the position of Au_{11} bound to subunit III places subunit III in the latter two domains rather than in the central domain.

A more detailed comparison of the Au_{11} binding site with images of unstained frozen hydrated cytochrome oxidase crystals requires us to determine which view or hand of the dimer imaged in Figure 5 should be compared with the view of the frozen hydrated dimer shown in, for example, Figures 3 and 6 of Frey and Murray (1994). The two views are mirror images of one another in two-dimensional projection and result from the molecular packing in this crystal form which presents molecules viewed from opposite directions along the 2-fold axis perpendicular to the membrane. We describe the two views of a cytochrome oxidase dimer found in Figure 5 as either "leaning right" as is the molecule at the origin of the *a* and *b* unit cell vectors or as "leaning left". Since projection images of negatively stained and of frozen hydrated molecules are very similar in appearance, it is logical to compare right leaning negatively stained molecules with right leaning frozen hydrated molecules. Valpuesta et al. (1990), however, found that in comparing their three-dimensional structures, the molecules which appeared to be leaning left in negatively stained projection images should be compared with those which appeared to be leaning right in images of frozen hydrated molecules. This is due both to an apparent rotation of molecules by 25° in negatively stained crystals compared to frozen hydrated crystals and to different contrast mechanisms. For example, the lipid bilayer spanning regions do not contribute contrast in negatively stained crystals but do contribute contrast in frozen hydrated crystals. With this in mind, we have indicated the position of the Au_{11} peak taken from a left leaning molecule in Figure 5 in an image of a right leaning frozen hydrated dimer shown in Figure 6. If cytochrome oxidase dimers are rotated clockwise by 25° in frozen hydrated crystals compared to negatively stained crystals as suggested by Valpuesta *et al* (1990), then the position in Figure 6 which more closely corresponds with the Au_{11} peak in Figure 5 would be that indicated by the Roman numeral III.

Does this location for subunit III agree with a role in assembly of the other subunits and stabilization of the dimeric form of the enzyme? Frey and Murray have recently published a study of frozen hydrated monomeric and dimeric crystal forms of cytochrome *c* oxidase. Their results revealed the arrangement of the two monomers comprising a dimer and the location of the cytochrome *c* binding site (Frey & Murray, 1994). As seen in Figure 6a, the dimer can be approximated in projection as a parallelogram with dimensions of 44 by 82 Å and an included angle of 80°. The monomer is less regular consisting of a linear arrangement of two large domains, M1 and M2, and a smaller domain, X, as shown in Figure 6b. The longest dimension of a monomer is approximately the same as the dimer, and in

forming a dimer the two monomers align with their long axes parallel and the X domain of one monomer partially overlapping in projection domain M2 of the other. Domains M1 of both monomers are close together at the dimer center and are not resolved in the images of dimers. As discussed above, the Au_{11} locus (and the site of subunit III) lies along the *a* axis approximately 30 Å from the center of the dimer, the region where domains M2 of one monomer and X of the other overlap. Thus, subunit III could indeed help stabilize the dimer form of the enzyme by forming intermolecular contacts with subunits from the neighboring monomer, but the two subunit III polypeptides in a dimer are too far apart to interact with each other. Is subunit III located in domain M2 or in X? Subunit III is readily removed from the cytochrome oxidase complex without loss of enzyme activity (Gregory & Ferguson-Miller, 1988; Nalecz et al., 1985; Prochaska & Fink, 1987; Thompson & Ferguson-Miller, 1983) and melts independently of the core enzyme as determined by high sensitivity differential scanning calorimetry (Morein et al., 1990). Domain X, is peripherally located, and one can imagine that it could be removed without seriously disrupting the structure of the rest of the enzyme. It is, however, marginally large enough to accommodate the seven transmembrane α-helices proposed for subunit III and is barely within 15 Å of the Au_{11} even after accounting for a 25° rotation of cytochrome oxidase molecules in frozen hydrated crystals relative to negatively stained crystals. Thus, at this time it seems more probable that subunit III is located in domain M2 although the alternative cannot be ruled out.

Cytochrome *c* binds to cytochrome oxidase via salt bonds between basic residues (primarily lysines) of cytochrome *c* and acidic residues of subunit II. The Lys residues involved in this interaction have been identified and lie on the surface of cytochrome *c* on which the heme is exposed while the acidic residues on cytochrome oxidase are all on subunit II. One of these acidic residues, Glu-198, lies between two cysteine residues which probably serve as ligands of Cu_A (Ferguson-Miller et al., 1978; Millett et al., 1983; Rieder & Bosshard, 1978; Smith et al., 1977) placing the heme of cytochrome *c* in proximity to Cu_A, the first acceptor of electrons from cytochrome *c* (Hill, 1991). Isoform-1 of yeast cytochrome *c* contains a cysteine at residue 107 which is exposed on the surface of the molecule opposite the side which binds to cytochrome oxidase subunit II, and Cys-115 of subunit III can be cross-linked to Cys-107 of yeast cytochrome *c* via a disulfide bond when it is bound at the high affinity site (Birchmeier et al., 1976; Fuller et al., 1981; Darley-Usmar et al., 1984). Capaldi et al. (1992) have proposed that in cytochrome oxidase dimers the high affinity binding site for cytochrome *c* lies in a cavity formed by subunit II of one monomer and subunit III of the other (Capaldi et al., 1982). Hall et al. have studied the topology of cytochrome oxidase by Forster energy transfer between an extrinsic fluorescence probe bound to subunit III and the heme of cytochrome *c* bound to the high affinity site on cytochrome oxidase. They concluded that in cytochrome oxidase dimers, subunit III of one monomer is relatively close (26−40 Å) to the cytochrome *c* binding site on subunit II of the other monomer, but within one monomer subunit III is more than 54 Å from the cytochrome *c* binding site (Hall et al., 1988). This supports the model for cytochrome *c* binding to cytochrome oxidase dimers proposed by Capaldi et al. (1982). Frey and Murray (1994)have identified the cytochrome *c* binding site on both monomers and dimers, and this site is indicated in the cytochrome oxidase dimer in Figure 6. The location of subunit III 30 Å from the center of the dimer suggests that subunit II must be near the center of the dimer as it binds to the surface of yeast cytochrome *c* opposite Cys-107. Furthermore, Estey and Prochaska (1993) have demonstrated that the two subunits I in a dimer can be cross-linked placing them close together at the 2-fold axis of the dimer. Thus, the large central domain composed of two domain M1's from two monomers probably contains the core subunits I and II which bind all of the catalytic metal centers.

The position of subunit III shown in Figure 6a is also consistent with the site of subunit IV previously determined from electron microscopy of crystals decorated with anti subunit IV Fab's, monovalent antibody fragments (Frey et al., 1985). The anti-IV Fab-decorated crystals showed two peaks of density each centered approximately 30 Å from the center of the dimer. Finel has found that in monomers, subunit IV and subunit III can be cross-linked with DSP [dithiobis(succinimidylpropionate)] and must, therefore, be very close together (Finel, 1989; Finel & Wikstrom, 1988). Based upon the results described above, Figure 6 proposes a model for the relative positions of subunits I, II, III, and IV and of the cytochrome *c* binding site in the two-dimensional projection of cytochrome oxidase dimers.

Two important questions remain unanswered by this study. The most significant is whether subunit III is associated with domain X or with domain M2. While our results interpreted in the context of the three-dimensional structures determined by Valpuesta et al. (1990) suggest that subunit III is associated with the M2 domain, a similar study of maleimide Au_{11} labeling of subunit III in the monomer crystal form of cytochrome *c* oxidase would confirm this interpretation. Such a study is currently underway in our laboratory. The second question is the location of Cys-115 of subunit III along the *z* axis normal to the plane of the membrane. Determining this will require recording and processing a large number of electron micrographs of tilted cytochrome oxidase dimer crystals labeled with maleimide undecagold at Cys-115 of subunit III so that the position of Au_{11} bound to Cys-115 can be identified by three-dimensional difference Fourier analysis. Once the location of Cys-115 of subunit III is established in three dimensions, we can determine where subunit III is in the three-dimensional reconstruction of frozen-hydrated cytochrome *c* oxidase dimers. This will help define the role of subunit III in the structure and function of cytochrome oxidase as well as help refine the site of cytochrome *c* binding and its orientation in the binding site.

ACKNOWLEDGMENT

We acknowledge the help of Bill Morris and Jim Varnell (SDSU College of Sciences Computer Support Group) for software used to scan micrographs and are grateful for the help of Dr. A. P. Somlyo (Department of Molecular Physiology and Biological Physics, University of Virginia School of Medicine) in energy dispersive X-ray analysis of individual crystals labeled with undecagold clusters. We also gratefully acknowledge the help and advice of Dr. Perry A. Frey.

REFERENCES

Anthony, G., Stroh, A., Lottspeich, F., & Kadenbach, B. (1990) *FEBS Lett. 277*, 97−100.

Buse, G., Meinecke, L., & Bruch, B. (1985) *J. Inorg. Biochem. 23*, 149−153.

Capaldi, R. A. (1990a) *Arch. Biochem. Biophys. 280*, 252−262.

Capaldi, R. A. (1990b) *Annu. Rev. Biochem. 59*, 569−596.

Capaldi, R. A., Darley-Usmar, V., Fuller, S., & Millett, F. (1982) *FEBS Lett. 138*, 1−7.

Costello, M. J., & Frey, T. G. (1982) *J. Mol. Biol. 162*, 131−156.

Crum, J., Gruys, K. J., Frey, P. A., & Frey, T. G. (1994) *Biophys. J. 66*, A8.

Deatherage, J. F., Henderson, R., & Capaldi, R. A. (1982a) *J. Mol. Biol. 158*, 501−514.

Deatherage, J. F., Henderson, R., & Capaldi, R. A. (1982b) *J. Mol. Biol. 158*, 487−499.

Estey, L. A., & Prochaska, L. J. (1993) *Biochemistry 32*, 13270−13276.

Ferguson-Miller, S., Brautigan, D. L., & Margoliash, E. (1978) *J. Biol. Chem. 253*, 149−159.

Finel, M. (1989) Ph.D. Thesis, University of Helsinki, Finland.

Finel, M., & Wikstrom, M. (1986) *Biochim. Biophys. Acta. 851*, 99−108.

Finel, M., & Wikstrom, M. (1988) *Eur. J. Biochem. 176*, 125−129.

Frank, J., Shimkin, B., & Dowse, H. (1981) *Ultramicroscopy 6*, 343−358.

Frey, T. G. (1994) *Microsc. Res. Tech. 27*, 319−332.

Frey, T. G., & Murray, J. M. (1994) *J. Mol. Biol. 237*, 275−297.

Frey, T. G., Chan, S. H. P., & Schatz, G. (1978) *J. Biol. Chem. 253*, 4389−4395.

Frey, T. G., Costello, M. J., Karlsson, B., Haselgrove, J. C., & Leigh, J. S. (1982) *J. Mol. Biol. 162*, 113−130.

Frey, T. G., Kuhn, L. A., Leigh, J. S., Costello, M. J., & Chan, S. H. P. (1985) *J. Inorg. Biochem. 23*, 155−162.

Fuller, S. D., Capaldi, R. A., & Henderson, R. (1979) *J. Mol. Biol. 134*, 305−327.

Georgevich, G., Darley-Usmar, V. M., Malatesta, F., & Capaldi, R. A. (1983) *Biochemistry 22*, 1317−1322.

Gregory, L. C., & Ferguson-Miller, S. (1988) *Biochemistry 27*, 6307−6314.

Hahn, T. (1983) in *International Tables for Crystallography* (T. Hahn., Ed.) pp 854, D. Reidel, Boston.

Hainfeld, J. F. (1988) *Nature 333*, 281−282.

Hall, J., Moubarak, A., O'Brien, P., Pan, L. P., Cho, I., & Millett, F. (1988) *J. Biol. Chem. 263*, 8142−8149.

Haltia, T., & Wikstrom, M. (1992) in *Molecular Mechanisms in Bioenergetics* (Ernster, L., Ed.) pp 217−239, Elsevier Science Publishers B.V., Amsterdam.

Haltia, T., Finel, M., Harms, N., Nakari, T., Raitio, M., Wikström, M., & Saraste, M. (1989) *EMBO J. 8*, 3571−3579.

Haltia, T., Saraste, M., & Wikström, M. (1991) *EMBO J. 10*, 2015−2021.

Henderson, R., Capaldi, R. A., & Leigh, J. S. (1977) *J. Mol. Biol. 112*, 631−648.

Henderson, R., Baldwin, J. M., Downing, K. H., Lepault, J., & Zemlin, F. (1986) *Ultramicroscopy 19*, 147−178.

Hill, B. C. (1991) *J. Biol. Chem. 266*, 2219−2226.

Kadenbach, B., Jarausch, J., Hartmann, R., & Merle, P. (1983) *Anal. Biochem. 129*, 517−521.

Lever, M. (1977) *Anal. Biochem. 83*, 274−284.

Malatesta, F., & Capaldi, R. A. (1982) *Biochem. Biophys. Res. Commun. 109*, 1180−1185.

McGeer, A., Lavers, G., & Williams, G. R. (1977) *Can. J. Biochem. 55*, 988−994.

Millett, F., de Jong, C., Paulson, L., & Capaldi, R. A. (1983) *Biochemistry 22*, 546−552.

Milligan, R. A., & Flicker, P. F. (1987) *J. Cell Biol. 105*, 29−39.

Milligan, R. A., Whittaker, M., & Safer, D. (1990) *Nature 348*, 217−221.

Morein, P. E., Diggs, D., & Freire, E. (1990) *Biochemistry 29*, 781−788.

Muller, M., & Azzi, A. (1985) *FEBS Lett. 184*, 110−114.

Nalecz, K., Bolli, R., & Azzi, A. (1983) *Biochem. Biophys. Res. Commun. 114*, 822−828.

Nalecz, K. A., Bolli, R., Ludwig, B., & Azzi, A. (1985) *Biochim. Biophys. Acta. 808*, 259−272.

Prochaska, L. J., & Fink, P. S. (1987) *J. Bioenerg. Biomembr. 19*, 143−165.

Rieder, R., & Bosshard, H. R. (1978) *J. Biol. Chem. 253*, 6045−6053.

Robinson, N. C., & Talbert, L. (1986) *Biochemistry 25*, 2328−2335.

Safer, D., Bolinger, L., & Leigh, J. S. (1986) *J. Inorg. Biochem. 26*, 77−91.

Saraste, M., Holm, L., Lemieux, L., Lübben, M., & van der Oost, J. (1991) *Biochem. Soc. Trans. 19*, 608−612.

Smith, H. T., Staudenmayer, N., & Millett, F. (1977) *Biochemistry 16*, 4971−4974.

Sone, N., & Kosako, T. (1986) *EMBO J. 5*, 1515−1519.

Suarez, M. D., Revzin, A., Narlock, R., Kempner, E. S., Thompson, D. A., & Ferguson-Miller, S. (1984) *J. Biol. Chem. 259*, 13791−13799.

Thompson, D. A., & Ferguson-Miller, S. (1983) *Biochemistry 22*, 3178−3187.

Valpuesta, J. M., Henderson, R., & Frey, T. G. (1990) *J. Mol. Biol. 214*, 237−251.

Wikstrom, M. (1977) *Nature 266*, 271−273.

Wikstrom, M., Krab, K., & Saraste, M. (1981) in *Cytochrome Oxidase: A Synthesis* Academic Press, London.

Yang, H., Reardon, J. E., & Frey, P. A. (1984) *Biochemistry 23*, 3857−3862.

Yang, Y.-S., Datta, A., Hainfeld, J. F., Furuya, F. R., Wall, J. S., & Frey, P. A. (1994) *Biochemistry* (in press).